Tetrahedron Vol. 49, No. 30, pp. 6533-6544, 1993
Printed in Great Britain

0040-4020/93 $6.00+.00

Conformation of Taxotere® and Analogues Determined by NMR Spectroscopy and Molecular Modeling Studies

Joëlle Dubois, Daniel Guénard*, Françoise Guéritte-Voegelein , Nourredine Guedira, Pierre Potier, Brigitte Gillet and Jean-Claude Beloeil.

Institut de Chimie des Substances Naturelles - CNRS 91198 Gif sur Yvette Cedex- France

(*Received in Belgium* 4 *January* 1993; *accepted* 19 *February* 1993)

Abstract : Taxol **1** and Taxotere ® **2** are antitumor compounds interacting with tubulin proteins. In order to find the best conformational fit to the receptor site, the structures of taxotere and twelve analogues showing various *in vitro* biological activity on tubulin, have been investigated by ^{1}H NMR spectroscopy and molecular modeling studies. These structures were compared to that of Taxotere ® **2** obtained by X-ray analysis. The results obtained from these studies suggest that the most active 2'R,3'S compounds possess a conformation in which the benzoate group at C-2 holds the side chain in a defined position due to hydrophobic interactions between this group and the N-amido or N-carbonyloxy group at C-3'. This situation together with the presence of hydrogen bonding between 2'OH -3'NH and 2'OH-1'C=O gives rise to a specific orientation of the hydroxyl and phenyl groups at C-2' and C-3'. On the other hand, the 2'S,3'R isomers which display low *in vitro* biological activity (ie: on tubulin), such as isotaxotere **8**, possess a different conformation with no hydrophobic interactions between the side chain and the taxan skeleton.

Since the discovery of taxol [1] and of its biological properties [2] a number of chemical and pharmacological studies have been performed on this antitumor diterpene, isolated from different species of the genus *Taxus*. Within the past ten years, taxol has become one of the most promising anticancer drugs based on results of Phase I and II clinical trials [3]. Taxol belongs to the spindle poisons family, and its unique mechanism of action involves promotion of the assembly of microtubules [2a]. Taxol binding to microtubules is highly specific, reversible and not temperature dependent [2a, 4].

As other taxan compounds (taxins and baccatins [5]), taxol **1** possesses a tricyclic carbon skeleton. In addition, taxol is characterized by the presence of an oxetan ring at carbons 4 and 5 and a 2'R, 3'S ester side chain at carbon 13 which mainly contributes to good receptor binding and, consequently, to the biological efficacy of the drug.

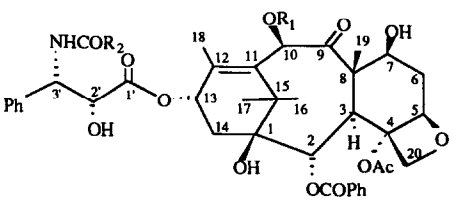

1 R_1 = Ac , R_2 = Ph

2 R_1 = H , R_2 = OtBu

Several routes to a total synthesis of taxol have been published [6] and a number of taxol analogues have been isolated from various species of *Taxus* or prepared by hemisynthesis from taxol itself or from

10-deacetyl baccatin III [7], a chemical precursor isolated from the leaves of the yew tree. Among these substances, taxotere **2** [8], has become a very promising anticancer agent [9]. Similarly to taxol **1**, taxotere **2** bears the (2'R, 3'S) threo configuration, but differs from the former by its substituents at C-10 and C-3'. In taxotere, the C-10 acetyl and C-3' benzamide groups of taxol are replaced respectively by a hydroxyl and a N-t-BOC group.

Early structure-activity studies showed that minor structural modifications of taxol could lead to great differences in binding to tubulin. Thus acylation of the 2' hydroxyl group leads to an inactive compound whereas hydrolysis of the C-10 acetyl group and acetylation of the C-7 hydroxyl group does not significantly modify the *in vitro* biological activity [10]. Other structural modifications performed on the side chain at carbon 13 showed that the nature and configuration[11,12] of the 2' and 3' carbons are important for the *in vitro* activity (i.e. antitubulin activity).

The first 3-dimensional structure of a related taxol analogue was obtained from the X-ray analysis of taxotere [13] and showed that the side chain adopts a particular geometry due to intramolecular hydrogen bonding (1' C=O -- 2'-OH, on one hand and 2'-OH -- NH on the other) [11,12]. The conformation of taxol has also been studied in hydrophobic solution by NMR spectroscopy [14] and molecular modeling studies [14d]. These studies led to the conclusion that the structure of taxol in solution is very similar to the structure of taxotere in the solid state.

In contrast to the rigid conformation of the taxan skeleton, the side chain at C-13 possesses a high degree of freedom and can thus adopt several conformations depending first on the nature and the configuration of its substituents at C-2' and C-3' and secondly on the surrounding medium. In order to define the most accurate conformational fit to the receptor site, the structures of taxotere and twelve analogues bearing different substituents at carbon 2' and 3' and showing different *in vitro* biological activity on tubulin, have been investigated by ^{1}H NMR spectroscopy and molecular modeling studies and compared to that of taxotere **2** obtained from X-ray analysis. We thus propose in this paper a set of active conformations for taxol-like compounds and the most optimal parameters for the binding process. The results described here are complementary to those obtained by Scott and Swindell[15].

EXPERIMENTAL

Chemistry

Taxol was isolated from the trunk bark of the yew tree *Taxus baccata* L.[16]. Literature references concerning the preparation and activity of compounds bearing different substituents and configurations at C-2' and C-3' are given in Table 2. Compounds **11**, **12** and **14** were prepared as follows and their structures were determined by NMR spectroscopy (see below) and mass spectra (recorded on an AEI MS9 (CI) or on a Kratos MS80 (FAB)).

2'-acetyltaxotere **11** : 750µmol of acetic anhydride were added to 75µmol of taxotere **2** in 2ml of dry pyridine at 0°C. The reaction mixture was stirred at 0°C for 4h. After hydrolysis the mixture was extracted with methylene chloride. The organic layer was washed twice with water, dried and concentrated. Purification by preparative TLC (CH_2Cl_2 / MeOH 95:5) gave 2'-acetyltaxotere **11** and 2',7-diacetyltaxotere in respectively 50% and 22% yield. ^{1}H NMR($CDCl_3$) δ 1.11(s,C-16H_3), 1.23(s,C-17H_3), 1.35(s,tBu), 1.75(s,C-19H_3), 1.85(m,C-6Hβ), 1.94(s,C-18H_3), 2.10(s,2'-OCOCH_3), 2,.18-2.28(m,C-14H_2), 2.44(s,4-OCOCH_3), 2.59(m,C-6Hα), 3.92(d,J=7,C-3H), 4.27(m,C-7H), 4.19-4.33(2d,J=8,C-20H_2), 4.97(d,J=9,C-5H),

5.31(s,C-10H), 5.37(bs,C-2'H), 5.44(bs,C-3'H), 5.69(d,J=7,C-2H), 6.23(t,J=8,C-13H), 7.30-7.37(m,C_6H_5), 7.50-7.60-8.11(m,$OCOC_6H_5$); MS-FAB$^+$ *m/z* 872(M+Na$^+$) 850(MH$^+$),549, 527, 509, 346, 327.

10-deacetylbaccatin III 13-(N-ethoxycarbonyl-(2'R,3'S)-3'-phenylisoserinate) **12** : 55µmol of diethyldicarbonate and 125µmol of sodium hydrogenocarbonate were added under argon to a solution of 7,10-bis(2,2,2-trichloroethyloxycarbonyl)-10-deacetylbaccatin III 13-((2'R,3'S)-3'-phenylisoserinate)[17] (50µmol) in 4ml ethyl acetate. The reaction mixture was stirred for 1h at room temperature. Ethyl acetate was added and the organic layer was washed twice with water, dried and concentrated. Purification by preparative TLC (CH_2Cl_2 / MeOH 96:4) afforded the 7,10 protected ethyloxycarbonyl derivative in 80% yield. Removal of the 7,10-protective groups [17] gave compound **12** in 64% yield after purification by preparative TLC (CH_2Cl_2 / MeOH 95:5) .^{1}H NMR($CDCl_3$) δ 1.17(bs,$OCH_2\underline{CH_3}$ and C-16H_3), 1.24(s,C-17H_3), 1.77(s,C-19H_3), 1.87(s,C-18H_3)1.89(m,C-6Hα), 2.22(m,C-14H_2), 2.35(s,$OCOCH_3$), 2.52(m,C-6Hß), 3.88(d,J=7,C-3H), 4.01(q,J=7,$OCO\underline{CH_2}CH_3$), 4.23(m,C-7H), 4.18-4.30(2d,J=8,C-20H_2), 4.62(bs,C-2'H), 4.93(d,J=9,C-5H), 5.21(s,C-10H), 5.25(bd, J=9,C-3'H), 5.64(d,J=7,C-2H), 5.86(bd,J=9,NH), 6.21(t,J=8,C-13H), 7.39(s,C_6H_5), 7.50-7.60-8.10(m,$OCOC_6H_5$) ; MS-CI *m/z* 780(MH$^+$), 762, 744, 527, 509, 491, 405, 387, 254, 208, 178.

2'-Acetyl-10-deacetylisotaxol **14** : 33µmol of 10-deacetylisotaxol **13** were acetylated in a mixture of 1ml pyridine and 0.1ml acetic anhydride during 0.5h at room temperature. After hydrolysis, the product was extracted with methylene chloride and the organic layer was washed twice with water, dried over sodium sulfate and concentrated. Purification by preparative TLC (CH_2Cl_2 / MeOH 95:5) gave 51% of pure **14** and 22% of 2',7-diacetyl-10-deacetylisotaxol. ^{1}H RMN($CDCl_3$) δ 1.13(s,C-16H_3) 1.21(s,C-17H_3) 1.78(s,C-19H_3) 1.86(m, C-6Hα) 1.98(s,C-18H_3) 2.14(s,4-OAc) 2.16(m,C-14H) 2.23(s,2'-OAc) 2.35(m,C-14H) 2.58(m,C-6Hß) 3.94(d,J=7,C-3H) 4.18 and 4.32(2d,J=8,C-20H_2) 4.25(m,C-7H) 4.95(d,J=9,C-5H) 5.22(s,C-10H) 5.45(d,J=2.5,C-2'H) 5.66(d,J=7,C-2H) 5.82(dd,J=2.5 and J=9,C-3'H) 6.19(t,J=8,C-13H) 7.26(d,J=9,NH) 7.35-7.70 (m, aromatic) 7.79(d,*o*-$NHCOC_6H_5$) 8.07(d,*o*-$OCOC_6H_5$) ; MS-FAB$^+$ *m/z* 876(M+Na+), 854(MH+), 527, 509, 328, 237.

NMR studies

NMR spectra were recorded on a *Bruker AM 400* spectrometer. The compounds were dissolved in deuterated solvants ($CDCl_3$ or CD_3OD, *CEA France*) to a final concentration of 75 mM. 7,10-diglycyltaxotere **15** (2mg) was dissolved in 1ml of D_2O.

The ROESY spectra were recorded either at 243K or 300K with a relaxation delay of 1s, 32 scans and a mixing time of 1s with 512 experiments of 2048 data points, sinebell-shifted by π/6 multiplication in both dimensions (sweep width of about 6000Hz). Quantitative internuclear proton-proton distances for taxotere **2** and isotaxotere **8** were obtained from NOESY[18] spectroscopy rather than ROESY[19], in which, quantification of cross peak intensities in terms of internuclear distances is complicated by the possibility of artefacts [20] . A series of 2D nOe spectra were recorded with parametric variation of the mixing time(τ_m). Using the two-spin approximation, the distance r_{AB} between proton A and B was deduced from the initial rate according to the equation $I_{AB}(\tau_m) \propto (\tau_c / r^6_{AB})\tau_m$ [21] where I_{AB} is the cross peak intensity and τ_c the correlation time. The cross-peak intensities were measured by volume integration [22], with the base plane correction and plotted versus τ_m. Distances data were calculated using the H7-H10 distance as reference (2.4Å based on the taxotere X-ray structure). As mentioned by Hilton *et al* [14c] the errors associated with the distance measurements were difficult to determine. The phase sensitive NOESY spectra for taxotere **2** were

recorded at 300K with a relaxation delay of 1s, 32 scans, and mixing times of 50, 100, 200, 300, 500, 700, 900 ms and 1s with 512 experiments of 2048 data points. Before Fourier transformation, the data were multiplied by squared cosine function in both dimensions. For isotaxotere **8**, the phase sensitive NOESY spectra were recorded at 300K with a relaxation delay of 5s, 8 scans and mixing times of 50, 100, 200, 400, 500 and 700 ms with 512 experiments of 2048 data points. The data obtained were then treated as for taxotere. A sweep width of 4000Hz was employed in both dimensions for all the NOESY experiments.

Molecular modeling

Molecular modeling were performed using MacroModel (version 3.1) [23], on a Silicon Graphics 4D/35 workstation. Starting structures were generated from the X-ray structure of taxotere[13] data and fully minimized using MM2 force field parameters. Conformational searches were performed using the Batchmin program (version 3.1) [23] with the Monte Carlo procedure or the systematic conformational search (60° increments) varying the dihedral angles of the C-13 side chain, the C-2 benzoate and the C-4 acetate groups. These experiments were performed in vacuo or in the presence of chloroform or water molecules, and without any NMR constraint. The use of a water surrounding seems to provide a more accurate structure of these compounds because hydrophobic interactions certainly control the conformation. The resulting conformers were analyzed using MacroModel or Insight (Biosym) in order to define the different families of conformers according to the dihedral angles of the side chain about C1'-C2', C2'-C3' and C3'-NH. The energetic classification of conformers was also validated using the semi-empirical molecular orbital program MOPAC (AM1 Hamiltonian).

RESULTS AND DISCUSSION

Conformation of Taxotere ®.

Crystals of taxotere **2** were obtained from methanol [13]. As mentioned above, the X-ray analysis of taxotere led to the conclusion that in the solid state, the side chain adopts a particular conformation due first to intramolecular hydrogen bonding (1'C=O -- 2'-OH, on one hand and 2'-OH -- NH on the other) and, secondly, to interactions between the substituents of the side chain and those of the taxane framework[11,12] (structure **2a**). Moreover, in the crystal lattice, hydrophilic and hydrophobic intermolecular interactions occur within a sphere of 2 Å radius. The hydrophilic interactions include the C-2' hydroxyl and the C-1' carbonyl groups of the side chain and the oxygenated functions at carbons 7, 9 and 10. The second set of interactions involves the C-2 benzoate of one molecule, the t-Boc group of another one and the C-4 acetyl of a third molecule. Consequently, it can be suggested that the driving force of the crystal arrangement is the result of the stacking of the molecules due to intermolecular hydrophobic interactions. A similar hypothesis can also be deduced from NMR results.

At room temperature, the ^{1}H-NMR spectrum of taxotere exhibits broadened singlets corresponding to the C-4 acetyl and C-3' t-butyl signals. A decrease or increase in the temperature enhances these signals without changing their chemical shifts. A similar effect was observed when the concentration decreased from 100 to 1 mg/ml in $CDCl_3$. These observed temperature and concentration dependencies can be interpreted as arising from the presence at high concentrations of two forms of taxotere: a free molecule and a complex of two molecules bound by their hydrophobic areas. Consequently, this can have an effect on the free rotation of the neighboring acetyl and t-butyl groups leading to the broadening of these groups. Despite

the hydrophobic character of chloroform, such hydrophobic interactions could take place. It must be pointed out that the ^1H NMR spectrum of the 7,10-diglycyl derivative **15** (see Table 2) in D_2O at low concentration (2mg/ml) led only to broadening of the t-butyl group. In this case, one can suggest that the free rotation of the t-Boc group is prevented because of intramolecular hydrophobic interactions between this group and the benzyl ring at C-2. This situation is in good agreement both with the X-ray structure and the molecular modeling studies.

Table 1. Comparison of Proton-Proton Distances from NOESY Experiments (300K, CD_3OD), Molecular Modeling Studies and X-ray Analysis for Taxotere **2** and Isotaxotere **8** [a,b].

	Taxotere **2**			Isotaxotere **8**	
Involved Protons	X-ray structure Structure **2a**	Molecular Modeling Conformer **2b**	NMR NOE	Molecular Modeling	NMR NOE
2-16	1.9	2.1	1.9	2.1	1.9
2-19	2.3	2.2	2.2	2.2	2.3
2-20	2.8	2.9	2.7	3.0	2.7
3-7	2.2	2.3	2.0	2.3	2.4
3-10	2.9	2.9	3.7	3.1	3,0
3-14	2.2	2.5	3.1	2.5	2.4
3-18	2.9	2.9	2.6	2.9	2.6
5-6α	2.0	2.3	2.1	2.3	2.3
5-20α	3.2	3.2	c	3.2	2.8
7-6α	2.3	2.4	2.7	2.4	2.5
7-10	2.4	2.4	2.4	2.4	2.4
10-18	2.2	2.1	2.2	2.1	2.2
13-17	1.6	1.9	2.0	2.0	2.0
13-18	3.1	3.0	2.8	2.9	d
16-19	2.7	2.5	2.9	2.6	d
19-20β	2.0	2.1	2.1	2.1	2.2
o-Bz2-OAc4	3.1	3.2	3.1	3.1	2.3
o-Bz2-20α	3.4	2.8	2.8	2.6	2.6
o-Phe3'-OAc4	2.7	2.5	2.8	5	e
2'-OAc4	4.0	2.9	2.6	1.9	2.4
3'-OAc4	2.6	2.2	2.8	4.0	e
2'-18	2.5	3.4	2.9	3.6	3.3
3'-18	4.0	4.6	e	2.5	2.5
2'-*o*-Phe3'	2.8	3.0	3.0	3.0	2.8
3'-*o*-Phe3'	2.4	2.4	2.9	2.3	2.5
2'-3'	2.3	2.4	2.7	2.5	2.6
Bz2-tBu	4.4	3.3	d	9.9	d

[a] Calculated distances are in Å. [b] For methyl groups involved in connectivities, distances from modeling studies were calculated between the nearest H. [c] not measurable because of the superposition of H5-H7 on H5-H20β NOE cross peaks. [d] buried under noise ridges. [e] cross-peaks were not observed.

The conformation of taxotere in solution was first studied using ROESY 2D NMR experiments rather than NOESY experiments because the taxane-type compounds show small NOE crosspeaks at the 400MHz spectrometer frequency. Similarly to taxol[14], the ROESY spectra of taxotere exhibits a number of cross peaks between the hydrogens of the taxenyl ring. In order to determine the conformation of taxotere in

solution , the interproton distances were determined by quantitative NOE studies using NOESY experiments (see experimental section).

The values reported in Table 1 were calculated by the initial buildup rates of nOe's. In some cases, second-order Overhauser effects (a process involving magnetization transfer through three sites) are suggested by the diagram of the τ_m dependence of the cross-peak intensity. This may explain the surprisingly high values obtained for the H3-H10 and H3- H14 taxan core distances when compared to the distances obtained from X-ray analysis and modeling studies.

When compared to the X-ray structure, the conformation of taxotere in solution shows a similar pattern of hydrogen bonding between the protons of the side chain. The main difference lies in the distance between the proton at 2' and the methyl groups Me18 and OAc4, suggesting a different position of the 2'-hydroxyl group.

The molecular modeling study of taxotere under various conditions (in chloroform, water or in vacuo) led to a low-energy conformer **2b** (-441.3 kcal). Similarly to the NMR results, the main difference between conformer **2b** and the X-ray structure **2a** (-431,6 kcal) is found in the orientation of the side chain hydroxyl group at C-2'. Moreover, when compared to the crystal structure **2a**, the benzoate group at C-2 of conformer **2b** is closer to the t-BOC group. This difference, shown in Figure 1, may be explained by the presence in the X-ray structure of **2a** of hydrophobic intermolecular interactions between the t-butyl and phenyl groups of neigboring molecules, whereas in **2b**, intramolecular proximity of the C-2 benzoate and C-3't-butyl group is favored.

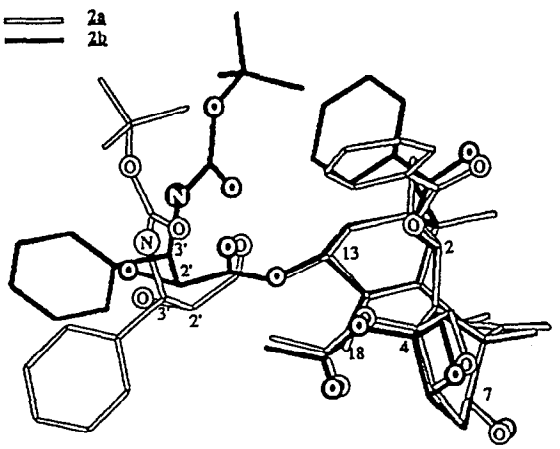

Figure 1 Overlay of taxotere structures **2a** (from X-ray analysis) and **2b** (from molecular modeling).

For taxotere, another conformer **2c** of higher energy is also generated. Structure **2c** exhibits a different pattern of hydrogen bonding occurring between the carbonyl group at C1' and the 3'NH. This lead to a trans situation for the 2' and 3' hydrogens. Molecular modeling of taxol in vacuo led to structure **2c** as the most stable conformer, whereas structure **2b** was only obtained in water. This difference between the two families of conformers **2b** and **2c** is also obtained from molecular modeling of the side chains devoid of the taxan moiety (heat of formation obtained by MOPAC: **2b**=-200.16 kcal, **2c** =-199.79 kcal).

Conformation of taxotere analogues 3-14.

We first compared the 1D ^{1}H-NMR spectra of taxol **1**, taxotere **2** and analogues **3-14** in order to determine the influence of the configuration at carbons 2' and 3' on the chemical shifts (Table 2). In $CDCl_3$ or CD_3OD, there is little effect of the solvant on the spectra. As previously reported [7] the only difference lies in the shape of the C-20H_2 signal that appears as a broad singlet in CD_3OD and as an AB quartet in $CDCl_3$. In contrast, a recent study [15] shows that taxol in aqueous solution produces a modification of the side chain conformation. Thus, the coupling constant $J_{H2'}$-$J_{3'H}$ increase from 2Hz in $CDCl_3$ to 8Hz in DMSO. Similarly, the ^{1}H-NMR spectra of taxotere in DMSO exhibits a coupling constant $J_{H2'}$-$J_{3'H}$ of 6Hz (data not shown).

The chemical shifts of the taxenyl ring protons of compounds **3-15** are similar to those of taxol **1** and taxotere **2**, except for the methyl group at C-18. Moreover, there exist some differences in the chemical shifts of H-2', H,-3' and the coupling constant $J_{H2'}$-$J_{3'H}$ (Table 2).

Table 2.NMR Assignments of Selected Protons (δ, ppm and J, Hz; 300K; $CDCl_3$) and *in vitro* Activity for Taxol, Taxotere and Analogues

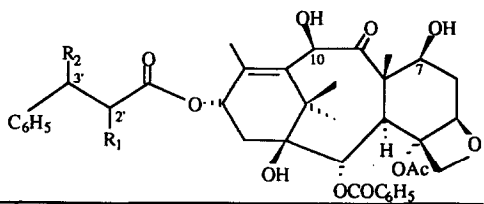

compound ref	R_1	R_2	δ H2'	δ H3'	J 2'-3'	δ $CH_3$18	ID_{50}/ID_{50}(taxol)[a]
1 (2'R,3'S)[b, 11]	OH	$NHCOC_6H_5$	4.76	5.76	2.6 Hz	1.78	1
2 (2'R,3'S)[11,17]	OH	$NHCO_2tBu$	4.62	5.26	bs[c]	1.87	0.5
3[17]	H	H	2.74	3.05	≈ 7 Hz	1.82	17
4 (2'R)[11]	OH	H	4.50	3.12	≈ 6 Hz	1.73	4.5
5 (2'S)[11]	OH	H	4.47	3.24-3.03	4,5 - 8 Hz	1.84	3.5
6 (3'S)[d,11]	H	$NHCO_2tBu$	2.93-3,10	5.18	6.3 - 6.8 Hz	1.72	2.3
7 (3'R)[d,11]	H	$NHCO_2tBu$	2.95	5.10	6 Hz	1.73	4.1
8 (2'S,3'R)[11,17]	OH	$NHCO_2tBu$	4.49	5.27	bs[c]	1.98	30
9 (2'S, 3'S)[d, 11]	OH	$NHCO_2tBu$	4.63	5.16	2.5 Hz	1.76	4.3
10 (2'R,3'R)[d 11]	OH	$NHCO_2tBu$	4.67	5.18	3.5 Hz	1.75	1.8
11 (2'R,3'S)	$OCOCH_3$	$NHCO_2tBu$	5.37	5.44	bs[c]	1.94	10
12 (2'R,3'S)	OH	$NHCO_2C_2H_5$	4.62	5.25	bs[c]	1.87	2.5
13 (2'S,3'R)[11,17]	OH	$NHCOC_6H_5$	4,66	5.74	2 Hz	1.98	4
14 (2'S,3'R)	$OCOCH_3$	$NHCOC_6H_5$	5.45	5.82	2.5 Hz	1.98	54
15 (2'R,3'S) [e,11]	OH	$NHCO_2tBu$	4.63	5.46	bs[c]	1.93	1.2

[a] ID_{50} is the concentration of product leading to 50% inhibition of the rate of microtubule disassembly. The ratio ID_{50}/ID_{50} (taxol) gives the activity with respect to taxol. [b] Taxol (unlike the other compounds the C10-OH group is acetylated). [c] bs: broad singlet, the coupling constant is not measurable. [d] Configurations at 2' and 3' were assigned from these NMR studies. [e] 7,10-diglycyl Taxotere.

Considering the threo compounds taxol **1**, 10-deacetyltaxol [24], taxotere **2**, isotaxotere **8** and 10-deacetylisotaxol **13**, a downfield shift of the Me-18 proton resonances seems to be related to a 2'S configuration. In addition, the downfield shift of the C18 methyl group is also associated with a small coupling constant between H2' and H3' (see compounds **2, 8, 11** and **12**). This may reflect a specific conformation of the side chain that is not observed in the erythro isomers **9** and **10**. It is also worth noting that the chemical shift of the Me-18 protons is influenced by the nature of the substituent at C3' only in the case of the (2'R,3'S) configuration (compare taxol **1**, 10-deacetyltaxol [21] and taxotere **2** with isotaxotere **8** and 10-deacetylisotaxol **13**). This effect is also observed when the 2' hydroxyl group is acetylated. Acetylation of taxotere **2** and 10-deacetylisotaxol **13** led respectively to compound **11** and **14**. Comparison of the NMR data shows that the Me18 signal of the (2'S,3'R) compounds **13** and **14** are similar whereas taxotere **2** exhibits a downfield shift of the methyl signal when compared to 2'-acetyltaxotere **11**. In contrast to the (2'R,3'S) and (2'S,3'R) threo isomers, careful analysis of the NMR data of erythro isomers **9** and **10** did not allow the assignment of the configuration at 2' and 3'.

The comparison of the NOE correlations between taxol **1**, taxotere **2** and compounds **3** to **14** led first to the conclusion that the presence of the side chain at C-13, regardless of its nature, has little effect on the conformation of the taxenyl ring. The differences observed in the NOE correlations of the various products lie essentially in the nature and configuration of the side chain leading to different conformations and positions with respect to the taxenyl ring. The NOE cross peak intensities between the protons of the side chain (H2' and H3') and those of the taxenyl ring (OAc4, $CH_3$18 and Ph3') are reported in table 3.

Table 3. Qualitative Aspect of Relative Intensities of NOEs for Taxol **1**, Taxotere **2** and Analogues **3-14** (ROESY, 300K, $CDCl_3$)

compounds	R1	R2	H2'/OAc4	H2'/Me18	H3'/Me18	H3'/OAc4	H2'/*o*-Ph3	*o*-Ph3'/OAc4
1 (2'R,3'S)	OH	$NHCOC_6H_5$	+++	+	0	+++	++	+
2 (2'R,3'S)	OH	$NHCO_2tBu$	+++	+	0	++	+	++
3	H		ε	0	0	ε	0	0
4 (2'R)	OH	H	+	ε	ε	ε	ε	ε
5 (2'S)	OH	H	++	0	0	+	++	++
6 (3'S)	H	$NHCO_2tBu$	+	0	0	ε	0	+
7 (3'R)	H	$NHCO_2tBu$	+	0	ε	ε	ε	+
8 (2'S,3'R)	OH	$NHCO_2tBu$	+++	0	++	0	+	0
9 (2'S,3'S)	OH	$NHCO_2tBu$	+	0	0	ε	ε	ε
10 (2'R,3'R)	OH	$NHCO_2tBu$	+	ε	0	ε	ε	0
11 (2'R,3'S)	$OCOCH_3$	$NHCO_2tBu$	++	ε	0	++	+++	++
12 (2'R,3'S)	OH	$NHCO_2C_2H_5$	+++	+	0	+++	+++	+++
13 (2'S,3'R)	OH	$NHCOC_6H_5$	++	0	++	+	+	0
14 (2'S,3'R)	$OCOCH_3$	$NHCOC_6H_5$	+++	0	++	ε	+	+

0 : no NOE; ε: very weak NOE; + :weak NOE; ++: moderate NOE; +++ : strong NOE

For most of the compounds, one observes a distinct NOE cross peak between H2' and OAc4. On the contrary, the H3'-OAc4 NOE signal intensity is weaker for compounds possessing the (2'S, 3'R) configuration. The 3' phenyl ring does not seem to participate in the side chain conformation but it is positioned close to the acetyl group, except for compound **12** which does not possess a bulky group at C- 3'. The most striking difference between the various compounds lies in the interaction of the side chain protons and the C-18 methyl group. Though not very important, the cross peak between H2' and Me18 is effective when the side chain possesses the (2'R,3'S) configuration. For compound **4**, one also observes a weak NOE cross peak suggesting that the 2'R configuration is responsible for that interaction. Similarly, the (2'R,3'R) configuration was assigned to compound **10**. Moreover, the absence of a cross peak between *o*-Ph3 and OAc4, observed only in 2'S,3'R compounds **8** and **13**, supports the (2'R, 3'R) configuration of compound **10**. On the other hand, the compounds that have a distinct cross peak between H3' and Me18 prove to have the (2'S,3'R) configuration, such as compounds **8**, **13** and **14**. Based on this fact, configuration 3'R was assigned to compound **7** because of the weak but distinct cross peak observed. It is worth noting that when compared to their related isomers , compounds possessing NOE connectivity between H3' and Me18 show the lowest activity : see **4** versus **5**, **7** versus **6**, **8** versus **2** and **13** versus taxol **1**. When compared to taxol **1** and taxotere **2**, the (2'S, 3'R) isomers **8** and **13** exhibit different noe correlations between the side chain and the taxan ring. As can be seen from tables 1 and 3, these differences involve mainly the 3'-18, 3'-OAc4 and Phe3'-OAc4 connectivities. This is consistent with a very different side chain orientation for **8** and **13**, also detected from molecular modeling studies.

Molecular modeling studies of taxol **1**, taxotere **2** and (2'R, 3'S) isomers performed in the presence of water always lead to a similar side chain skeleton to that of taxotere obtained from X-ray analysis. The only difference is that the substituents at C2' and C3' adopt different positions depending on their configuration. In the erythro analogues **9** and **10**, which possess good *in vitro* activity when compared to the threo analogue isotaxotere **8** (Table 3), a conformational reorientation enables the 3' phenyl group to replace the t-Boc group of conformer **2**. By contrast, this situation is not observed with isotaxotere **8**. Molecular modeling studies of compounds **3** , **4** and **6** show that they possess a similar conformation to that of taxotere **2b**. This result is in accordance with the fact that the gain in activity between an analogue without any substitution at 2' and 3' such as **3** and taxotere **2** is the product of the separate contributions brought by each substituents at carbons 2' and 3' (**4** and **6**). Surprisingly, the 2'-acetyl derivative **11**, which binds very weakly to tubulin, possesses a similar conformation to that of taxotere. Consequently, the decrease in activity can only be due to the loss of hydrophilic interactions involving the 2'-hydroxyl group and a polar group of the receptor site.

A more interesting observation concerns the structure of isotaxotere **8** and 10-deacteyl isotaxol **13** bearing the unnatural (2'S,3'R) configuration. The inversion of the side chain configuration led to less active compounds, but not to the same extent. Isotaxotere **8** is indeed 60 times less active than taxotere **2** whereas 10-deacetylisotaxol **13** is 4 times less active than taxol **1**. Molecular modeling studies showed that the most stable conformer of **8** and **13** differ from each other. If the lowest energy conformer **2b** of taxotere and 10-deacetylisotaxol **13** are compared, there exists a good superposition of the two structures except for the 2'-OH groups which are in opposite directions (Figure 2). Thus, the conformation of **13** resembles very closely that of 2'- deoxytaxotere **6** and **7**. This explains the similar *in vitro* activity found for compounds **6, 7** and **13**. In contrast, the side chain conformation of isotaxotere **8** is quite different. Consequently the binding of isotaxotere **8** to the receptor is weaker.

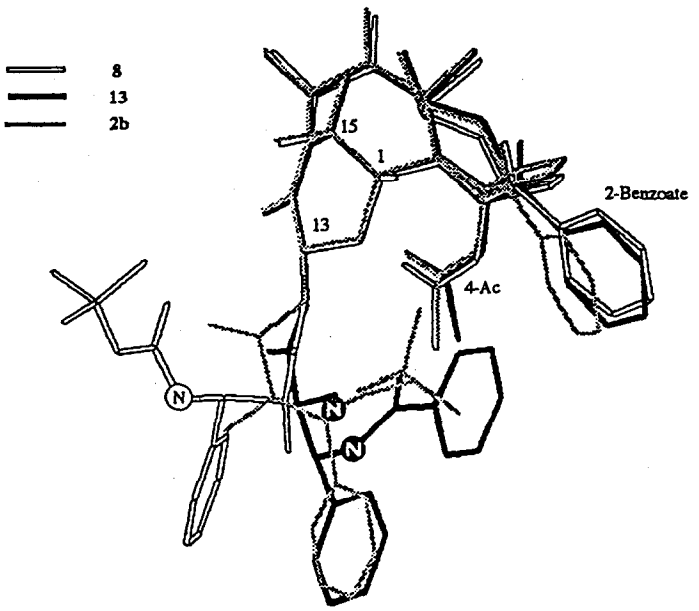

Figure 2. Comparison of the Taxotere conformer **2b** and the most stable conformation of Isotaxotere **8** and 10-Deacetylisotaxol **13**.

Although the stacking of the molecules in the crystal could resemble the interactions of a drug with its receptor, the conformation recognized by the receptor is certainly closer to the structure **2b** than **2a**. The results obtained from these studies suggest that the most active (2'R,3'S) compounds possess a conformation in which the benzoate group at C-2 holds the side chain in a definite position due to hydrophobic interactions involving this group and the N-amido or N-carboxyloxy group at C-3'. This situation, together with the presence of hydrogen bonding between 2'OH -3'NH and 2'OH-1'C=O has an influence on the position of the hydroxyl and phenyl groups at C-2' and C-3'. On the other hand, the (2'S,3'R) isomers, such as isotaxotere **8**, having low *in vitro* biological activity (ie: on tubulin), possess a different conformation with no hydrophobic interactions between the side chain and the taxan skeleton.

In the binding process to tubulin, we suggest that the taxan core of taxol-like compounds is first recognized (10-deacetylbaccatin III and baccatin III, which does not possess a side chain at C-13, have a low but distinct activity on microtubules[25]). Secondly, hydrophobic interactions occurring between the benzoate group at C-2 and the amino substituents at C-3' set the side chain in such a position that the hydroxyl and phenyl groups at respectively C-2' and C-3' can interact with tubulin residues leading to a stabilization of the drug-receptor binding. On the other hand, the C-7,9,10 oxygenated functions do not seem to participate to the binding process. This hydrophilic area is certainly outside the binding site, close to the biophase.

ACKNOWLEDGMENTS

We would like to thank Dr. R. Dodd for his help in the preparation of this paper. This work was supported by Grants from Rhône-Poulenc Rorer and the Ministère de la Recherche et de la Technologie of the French Government.

REFERENCES AND NOTES

1 Wani, M.C.; Taylor, H.L.; Wall, M.E.; Coggon, P.; McPhail, A.T. *J.Am.Chem. Soc.* **1971**, *93*, 2325

2 a) Schiff, P. B.; Fant, J.; Horwitz, S. B. *Nature* **1979**, *277*, 667. b) Hartwell, J.L. *Cancer Treat. Rep.*, **1976**, *60*, 1031

3 Rowinski, E. K.; Donehower, R. C. *Pharm. Ther.* **1991**, *52*, 35

4 Takoudju, M.; Wright, M.; Chenu, J.; Guénard, D.; Guéritte-Voegelein, F. *F.E.B.S.Letters*, **1988**, *227*, 96

5 Miller, R.W. *J. Nat.Prod.*, **1980**, *43*, 425

6 a) Blechert, S.; Guénard, D. *Taxus* Alkaloids in *The Alkaloids. Chemistry and Pharmacology*; Brossi, A., Ed; Academic Press: San Diego, 1990; Vol 39, pp 195-238. b) Swindell, C.S.*Org. Prep. Proced. Int.* **1991**, *23*, 465

7 Kingston, D.G.I. *Pharmac.Ther.* **1991**, *52*, 1

8 Colin, M.; Guénard, D.; Guéritte-Voegelein, F.; Potier, P. Eur.Pat.Appl.EP 253,378 (Cl.C07D305/14), 20 Jan 1988, FR Appl.86/10,400, 17 Jul 1986 *Chem.Abstr.* **1988**, *109*, 22762w

9 Bissery, M-C.; Guénard, D.; Guéritte-Voegelein, F.; Lavelle, F.*Cancer Research*, **1991**, *51*, 4845

10a) Parness, J.; Kingston, D.G.I.; Powell, R.G.; Harracksingh, C.; Horwitz, S.B. *Biochem.Biophys.Res.Comm.*, **1982**, *105*, 1082 b) Mellado, W.; Magri, N.F.; Kingston, D.G.I.; Garcia-Arenas, R.; Orr, G.A.; Horwitz, S.B. *Biochem.Biophys.Res.Comm.*, **1984**, *124*, 329

11Guéritte-Voegelein, F.; Guénard, D.; Lavelle, F.; Le Goff, M-T.; Mangatal, L; Potier, P. *J. Med. Chem.* **1991**, *34*, 992-998

12Swindell, C.S.; Krauss, N.E.; Horwitz, Ringel, I. *J. Med. Chem.*, **1991**, *34*, 1176-1184

13Guéritte-Voegelein, F.; Mangatal, L.; Guénard, D.; Potier, P.; Guilhem, J.; Cesario, M.; Pascard, C. *Acta Cryst.***1990**,*C46*, 781-784

14 a) Falzone, C.J.; Benesi, A.J.; Lecomte, T.J. *Tetrahedron Lett*, **1992**, *33*, 1169 b) Chmurny, G.N.; Hilton, B.D.; Brobst, S.; Look, S.A.; Witherup, K.M.; Beutler, J.A. *J.Nat.Prod.*, **1992**, *55*, 414 c) Hilton, B.D.,Chmurny, G.N.; Muschik, G.M. *J.Nat.Prod.*, **1992**, *55*, 1157 d) Baker, J.K. *Spectros.Lett.*, **1992**, *25*, 31

15 We thank Prof. Scott and Dr Swindell for sending us a manuscript of their work on NMR and molecular modeling studies of the conformation of taxol and of its side chain methylester in aqueous and non-aqueous solution: Williams, H.J.; Scott, A.I.; Dieden, R.A.; Swindell, C.S.; Chirlian, L.E.; Franci, M.M.; Heerding, J.M.; Krauss, N.E, *Tetrahedron*, this issue.

16 Sénilh, V.; Blechert, S.; Colin, M.; Guénard, D.; Picot, F.; Potier, P.; Varenne, P. *J.Nat.Prod.*, **1984**, *47*, 131

17Mangatal, L.; Adeline, M-T.; Guénard, D.; Guéritte-Voegelein, F.; Potier, P.*Tetrahedron*, **1989**, *45*, 4177

[18]Jeener, J.; Meier, B.H, Bachman, P.; Ernst R. *J.Chem.Phys,* **1979**, *71*, 4546

[19]Bax, A.; Davis, D.G. *J.Magn.Res,* **1985**, *63*, 207

[20]Homans, S.W. in *"A dictionary of concepts in NMR"*, Clarendon Press, Oxford, 1989

[21]Ernst, R.R.; Bodenhausen, G.; Wokaun, A. in *"Principles of Nuclear Magnetic Resonance in One and Two Dimensions"*, Oxford Science Publications, 1987

[22]We thank Dr. H.E.Quiniou for expert technical assistance in developing the spectral analysis software (on 38633 Compaq computer).

[23]Mohamadi, F.; Richards, N.G.J.; Guida, W.C.; Liskamp, R.; Lipton, M.; Caufield, C.; Chang, G.; Hendrickson, T.; Still, W.C.J. *Comp. Chem*, **1990**, *11*, 440

[24] McLaughlin, J.L.; Miller, R.W.; Powell, R.G.; Smith Jr, C.R. *J.Nat.Prod,* **1981**, *44*, 312

[25] Senilh, V.; Blechert, S.; Colin, M.; Guénard, D.; Picot, F.; Potier, P.; Varenne, P. *J.Nat.Prod.*, **1984**, *47*, 131